Review

Geochemistry, Mineralogy and Microbiology of Molybdenum in Mining-Affected Environments

Francesca Frascoli [1] and Karen A. Hudson-Edwards [2],* ID

[1] Department of Earth and Planetary Sciences, Birkbeck, University of London, Malet St., London WC1E 7HX, UK; francesca.frascoli@gmail.com
[2] Environment and Sustainability Institute and Camborne School of Mines, University of Exeter, Penryn, Cornwall TR10 9FE, UK
*   Correspondence: k.hudson-edwards@exeter.ac.uk; Tel.: +44-1326-259-489

Abstract: Molybdenum is an essential element for life, with growing production due to a constantly expanding variety of industrial applications. The potentially harmful effects of Mo on the environment, and on human and ecosystem health, require knowledge of Mo behavior in mining-affected environments. Mo is usually present in trace amounts in ore deposits, but mining exploitation can lead to wastes with very high Mo concentrations (up to 4000 mg/kg Mo for tailings), as well as soil, sediments and water contamination in surrounding areas. In mine wastes, molybdenum is liberated from sulfide mineral oxidation and can be sorbed onto secondary Fe(III)-minerals surfaces (jarosite, schwertmannite, ferrihydrite) at moderately acidic waters, or taken up in secondary minerals such as powellite and wulfenite at neutral to alkaline pH. To date, no Mo-metabolising bacteria have been isolated from mine wastes. However, laboratory and in-situ experiments in other types of contaminated land have suggested that several Mo-reducing and -oxidising bacteria may be involved in the cycling of Mo in and from mine wastes, with good potential for bioremediation. Overall, a general lack of data is highlighted, emphasizing the need for further research on the contamination, geochemistry, bio-availability and microbial cycling of Mo in mining-affected environments to improve environmental management and remediation actions.

1. Introduction

Molybdenum (Mo) is one of a number of 'strategic metals' that are necessary components for modern technologies and industries, but which may be subject to supply disruption. Molybdenum is most commonly used to make alloy steels and superalloys, but is also incorporated into catalysts, lubricants, pigments and as a refractory metal [1]. Grades of Mo in mined ore deposits generally range between 0.10% and 0.25% [2]. Molybdenum is mined as a primary product of Mo porphyry deposits, and as a by-product of Cu porphyry and other types of Cu-bearing ores [1]. Global mine production of Mo is on the order of just over 200,000 tons [3], with China being the largest producer (c. 35%–40% of world production), followed by Chile (c. 22%–23% of world production) and the US (c. 14%–20% of world production) [3].

Although Mo is an essential trace element for human health [4,5], it can be toxic in high doses. Animals and plants can also suffer from exposure to, and uptake of, high amounts of Mo, as well as Mo deficiencies [5]. Since mining and mine wastes are sources of Mo to the environment, they represent a pathway for Mo exposure. To provide information for assessing such pathways, in this paper we review the geochemistry, mineralogy and microbiology of Mo in mine wastes, describing the occurrence and controls on Mo uptake and mobility in affected waters, soils, sediments, plants, animals, minerals and microbes. We also outline areas for future research on Mo in mining-affected environments.

2. Geochemistry of Molybdenum in Mine Wastes

2.1. Molybdenum in Mine Waste Waters

Smedley and Kinniburgh [5] provide a comprehensive review of Mo in natural waters, including some mining-affected waters. In this section we extend this work by providing further examples of Mo concentrations in mining-affected waters (Table 1), including groundwaters, river waters and tailings pore waters. The highest aqueous Mo concentrations shown in Table 1, at >2 million µg/L, are those for laboratory-derived deionized water extractions of wastes from the Nowa Ruda Coalfield Mine, Silesia Basin, in south-west Poland [6]. The highest aqueous Mo concentrations shown in Table 1 for natural waters, between 10,400 and 13,900 µg/L, are from acid and acid to alkaline mine drainage water at the San Telmo mine in the Spanish Iberian Pyrite Belt, and at the Antamina mine in Peru [7,8]. Mo concentrations in tailings impoundment channel waters of Cu porphyry mines in the Machalí Cachapoal Province, Chile, are also high (2670–3900 µg/L) [9], as are those at the Sherridon Zn-Cu-Au-Ag mine, Canada (<5–1100 µg/L [10]) and at the Green Creek Zn-Ag-Pb-Au mine in Alaska (<5–1900 µg/L [10]). Tailings pore water Mo concentrations at the Ylöjärvi Cu-W-As mine in Finland and at the Nickel Rim Ni-Cu mine in Sudbury, Canada, are lower than those at the Cu porphyry and Zn-Cu-Au-Ag mines (1.28–209 µg/L and <0.005 µg/L, respectively) [10,11]. Groundwaters in the vicinity of the Ylöjärvi Cu-W-As mine in Finland and Au-Ag-Pb-Zn-As mines in the San Antonio-El Triunfo district in Mexico are elevated (<5–150 µg/L and 32.3 µg/L, respectively) [11,12]. These concentrations are higher than those in river waters in near the Laver Cu-Ag-Au mine in Sweden and the Gyama Cu-polymetallic mine in central Tibet (<0.3 µg/L and 0.6–9.7 µg/L, respectively) [13,14]. These mining-affected Mo aqueous concentrations exceed those for average rivers (8.0 nmol·kg^{-1}, [15]) and oceans (105 nM, [16]) by orders of magnitude. Greber et al. [17] attribute high Mo concentrations in Cu-Mo mines to the high solubility of Mo in water, even at very low oxygen concentrations.

Few guidelines exist for Mo in waters, but those available for drinking, irrigation, surface and ground water are summarized in Table 1. These range from 5 to 100,000 µg/L, with more stringent values applied for drinking and irrigation waters, and less stringent values for groundwaters around uranium sites. Smedley and Kinniburgh [5] point out that, although the fourth edition of the World Health Organisation's (WHO's) Guidelines for Drinking-Water Quality [18] advises a health-based value of 70 µg/L, they no longer have a guideline for Mo because concentrations as high as this are rarely found in waters designated for drinking. Most of the mining-affected ground and river water Mo concentrations shown in Table 1 do not exceed the guideline values. The tailings pore waters, and acid mine drainage waters, however, exceed most of the drinking and irrigation guidelines by one to two orders of magnitude, but they do not exceed the groundwater uranium mine standard. The fate of Mo in these mine wastes and environment is strongly determined by the behaviour of molybdate, since this is the main molybdenum species under pH > 4 and oxic and suboxic conditions [19].

Studies of stable isotope geochemistry have provided important insights into the cycling of metallic elements in mine wastes (e.g., [20]). Skierszkan et al. [8] attempted to determine whether stable isotopic Mo variations in mine waste rock drainage at the Anamina mine, Peru, gave information on Mo attenuation processes. δ^{98}Mo compositions of the mine drainage were heavier than (0.89‰ ± 1.25‰, 2 SD, n = 16), but overlapped somewhat with, δ^{98}Mo data for molybdenites and waste rock (0.13‰ ± 0.82‰, 2 SD, n = 9) (Figure 1). As a result, the authors suggested that the data were inconclusive, but suggested possible dissolution, adsorption and uptake of Mo (likely from anionic molybdate in solution [19]) in secondary minerals controlled Mo mobility. They stressed the need for fundamental research on the mechanisms of Mo isotope fractionation to aid interpretation of Mo mobility in mine waste and other environments.

Table 1. Concentrations of Mo in mining-affected waters.

| Mine	Ore Type	Mine Activity	Type	Mean or Range Mo Concentration (µg/L)	Reference
13 historic mines within the San Antonio-El Triunfo district, Mexico	Au-Ag-Pb-Zn-As	1878–1911	Groundwater	<5–150	Wurl et al. [12]
Ylöjärvi mine, Finland	Cu-W-As	1943–1966	Groundwater 8.4 m from tailings surface	32.3	Parviainen et al. [11]
Laver mine, Sweden	Cu-Ag-Au	1936–1946	Gräbergsbäcken brook, 2004–2005, dissolved fraction (<0.22 µm)	0.3	Alakangas et al. [13]
Gyama Cu-polymetallic plant, central Tibet	Cu-polymetallic	mid-15th century; 1990–present	River water	0.6–9.7	Huang et al. [14]
Balya mine, Turkey	Pb-Zn-Ag	early 1880s–late 1940s	Kocacay river water arid	1.12; 1.28	Aykol et al. [21]
San Telmo mine, Iberian Pyrite Belt, Spain	Cu	1970–1989	Acid mine drainage, leachate, pH 0.16–0.82	10,400	Sánchez-España et al. [7]
Antamina mine, Peru	Cu-Zn-Mo	2002–present	Mine drainage, pH 2.2–8.4, median 7.9	10–13,900	Skierszkan et al. [8]
Machalí, Cachapoal Province, Chile	Cu porphyry	1819–present	Tailings impoundment channel water	2670–3900	Smuda et al. [9]
Nickel Rim mine, Sudbury, Canada	Ni-Cu	1953–1958	Tailings pore water	<0.005	Lindsay et al. [10]
Ylöjärvi mine, Finland	Cu-W-As	1943–1966	Tailings pore water	1.28–209	Parviainen et al. [11]
Greens Creek mine, Alaska, USA	Zn-Ag-Pb-Au	1989–1993; 1996–present	Vadose zone pore-water; tailings pore-water	<5–15; <5–1900	Lindsay et al. [10]
Sherridon mine, Manitoba, Canada	Zn-Cu-Au-Ag	1930–1932; 1937–1951	Tailings pore water	<5–1100	Lindsay et al. [10]
Nowa Ruda Coalfield mine, Poland	Coal	n.r.	Deionised water extracts of mine waste	2,332,000	Chudy et al. [6]
Guideline values for Mo					
	Type of limit	Value (µg/L)	Organisation	Reference	
	Drinking water	70	World Health Organization	WHO [18]	
	Irrigation water in all soils	5	US Department of the Interior	US Department of the Interior [22]	
	Surface water	70	SEPA & AQSIQ, China	SEPA & AQSIQ [23]	
	Protection of aquatic life in freshwater	73	Canada	CCME [24]	
	Groundwater standard for inactive uranium mines	100,000	US EPA	US EPA [25]	
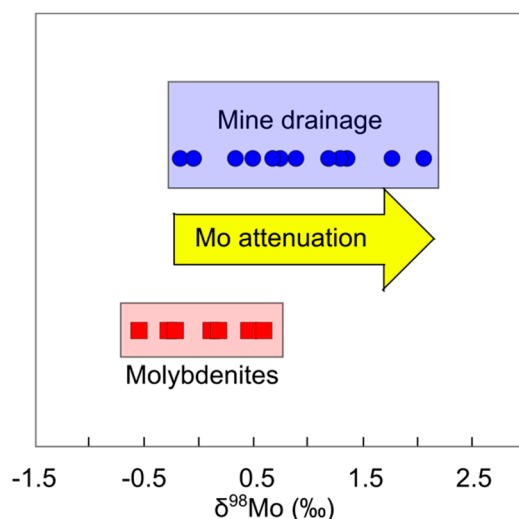
Figure 1. Molybdenum isotopic compositions of mine waste rock drainage and waste rock at the Antamina mine, Peru. δ^{98}Mo data are reported relative to NIST-SRM-3134 = +0.25‰. Reprinted (adapted) from Skierszkan et al. [8], with permission from Elsevier.

2.2. Molybdenum in Tailings and Mining-Affected Soils and Sediments

Varying concentrations of Mo for mine tailings and related materials have been documented (Table 2). Concentrations are low in Knaben Mo mine tailings (51 mg/kg Mo) and in tailings for deposits in which Mo is not the main commodity extracted (<100 mg/kg Mo; Au-Ag-Te Apuseni mine, Romania; Cu-Au-Ag Laver mine, Sweden; Cu-Zn Kristineberg mine, Sweden; Zn-Ag-Pb-Au Green Creeks mine, Alaksa). Copper- and Co-Mo porphyry mines generate tailings with higher Mo concentrations (100–300 mg/kg Mo), as shown for several sites in Chile (Table 2). The Mo concentrations (148 mg/kg Mo) in the massive sulfide Cu San Telmo deposit in the Iberian Pyrite Belt, Spain, is also within this range. The highest Mo concentrations recorded (3985 mg/kg Mo) are for tailings from the processing of Cu-polymetallic ores (including Cu porphyry ores) in the Gyama valley, central Tibet [14].

Examples of Mo concentrations in mining-affected soils and sediments are summarized in Table 3. For most of these, the Mo concentrations exceed those for uncontaminated soils (<10 mg/kg [5]) and upper continental crust (1.1 mg/kg, [26]). Exceptions include soils more than 250 m from the Portuguese Neves Corvo Cu-Pb-Zn mine [27], mine tailings and soils from the Portugues Ervedoa Sn-As mine [28] and rhizosphere soil around the Spanish Panasqueira Sn-W mine [29]. These low concentrations may be due to the distance from the mine, or to low Mo concentrations in the original mine materials and background soils.

The other documented Mo soil and sediment concentrations exceed 10 mg/kg, but are no higher than 138.9 mg/kg ([30]; Table 3). Interestingly, concentrations for soils and sediments associated with mines that specifically extract Mo are no higher than those that extract Cu and other metals. The highest Mo concentrations found were those for sediment associated with Cu concentration plant effluents, at 1950 mg/kg Mo [31].

Table 2. Concentrations of Mo in mine tailings. n.r.: not reported.

Mine	Ore Type	Mine Activity	Type	Mean Concentration (mg/kg)	Reference
Apuseni mine, Romania	Au-Ag-Te epithermal	1986–2006	Primary non-oxidised tailings	12	Sima et al. [32]
Carén tailings impoundment, Machalí, Cachapoal Province, Chile	Cu porphry	1819–present	Cemented tailings	101	Smuda et al. [9]
La Andina mine, Chile	Cu porphyry	1970–1980	Tailings in E2 impoundment	278	Dold and Fontboté [33]
Chuquicamata mine, Chile	Cu porphyry	n.r.	Fresh tailings solids	260	Smuda et al. [34]
Caletones smelter and unused Baraho, Chile	Cu-Mo porphyry	16th century; 1905–present	Tailings sediments	179	Kelm et al. [35]
Laver mine, Sweden	Cu-Au-Ag	1936–1946	Oxidized zone tailings (0–99 cm); unoxidised zone tailings (100–130 cm)	38.3; 24.3	Perez Rodriguez et al. [36]
San Telmo mine, Iberian Pyrite Belt, Spain	Cu	1970–1989	Tailings	148	Sánchez-España et al. [7]
Gyama valley, central Tibet	Cu-polymetallic	Mid-15th century; 1990–present	Tailings	3985	Huang et al. [14]
Kristineberg mine, Sweden	Cu-Zn	Unknown–early 1950s	Oxidized tailings; unoxidized tailings	17.7; 24	Holmstrom et al. [37]
Knaben mine, Sweden	Mo	1918–1973	Tailings pond	51	Langedal [38]
Greens Creek mine, Alaska, USA	Zn-Ag-Pb-Au	1989–1993; 1996–present	Tailings	49.5–76.3	Lindsay et al. [39]

Table 3. Concentrations of Mo in mining-affected soils and sediments. n.r.: not reported.

Mine	Ore Type	Mine Activity	Type	Mean or Range Concentration (mg/kg)	Reference
6th Region of Chile	Cu	n.r.	Soil 2 km from tailings impoundment	74	Garrido et al. [40]
Sarcheshmeh mine, Iran	Cu	Unknown–present	Top 0–5 cm soil around slag dump	19.4–138.6	Khorasanipour & Esmaeilzadeh [30]
Neves Corvo mine, Portugal	Cu-Pb-Zn	1988–present	Soils <250 m from mine	3.76	Farago et al. [27]
Globe-Miami mining district, Arizona, USA	Cu and other metals	n.r.	Soil	112	Haque et al. [41]
Powder River Basin, Wyoming, USA	Coal	n.r.	Soil near mine sites	13.5–20	Wang [42]
Ervedosa mine, Portugal	Sn-As	Phoenician, Roman, 1928–1969	Mine tailings and soils	5.91	Favas et al. [28]
Panasqueira mine, Spain	Sn-W	1896–present	Rhizosphere soil	0.6	Candeias et al. [29]
Knaben Mo mines, Sweden	Mo	1918–1973	Top section of overbank sediments	137	Langedal [38]
Knaben Momines, Sweden	Mo	1918–1973	0–25 cm floodplain sediments	60	Langedal [38]
Knaben Mo mines, Sweden	Mo	1918–1973	Sandbars	93	Langedal [38]
Gyama Cu-polymetallic plant, central Tibet	Cu-polymetallic	mid-15th century; 1990–present	Sediment	9.1–20.1	Huang et al. [14]
Mezica mining district, Slovenia	Pb-Zn	300 years up to 1995	River sediments	130	Miller & Gosar [43]
Sarcheshmeh mine, Iran	Cu	n.r.	Sediment associated with concentration plant effluents	1950	Khorasanipour et al. [31]

2.3. Molybdenum in Mining-Affected Plants

A limited number of studies have reported concentrations of Mo in mining-affect plants (Table 4). Farago et al. [27] analyzed the Mo concentrations in the tops of *Cistus* species and leaves and twigs of *Quercus rotundifolia* near to, and 12 km from, the Neves Corvo copper mine in southern Portugal. These concentrations were compared to 'available' Mo in soils that the plants grew on, which was analysed using ethylenediaminetetraacetic acid (EDTA) chemical extractions. Both EDTA-extracted soil Mo and plant Mo concentrations were low. Based on these results, both plants were proposed to be excluders of Mo.

Concentrations of Mo in roots and shoots of desert broom (*Baccharis sarothroides*) collected in the Globe-Miami mining district in Arizona were significantly higher than those at the Neves Corvo mine (Table 4). The *Baccharis sarothroides* grows on copper- and other metal-bearing tailings impoundments, and soils near these impoundments, in many sites near Claypool in south-central Arizona. Comparisons of Mo concentrations in soils and plants suggested that Mo was efficiently translocated from soils to roots and then to shoots, probably as the anionic molybdate [19]. The fact that the *Baccharis sarothroides* thrived on the Mo-rich soils and tailings suggested that was able to detoxify the Mo, and thus had good phytoremediation potential.

Table 4. Concentrations of Mo in mining-affected plants.

Mine	Ore Type	Type	Mean or Range Mo Concentration (mg/kg)	Reference
Globe-Miami mining district, Arizona, USA	Cu and other metals	Roots of desert broom (*Baccharis sarothroides*)	73.9	Haque et al. [41]
		Shoots	105.8	
Neves Corvo mine, Portugal	Cu-Pb-Zn	Quercus leaves	0.29–1.1	Farago et al. [27]
		Quercus twigs	0.34–0.98	
		Cistus tops	0.35–1.08	

3. Mineralogy of Mo in Mine Wastes

Molybdenum is widely distributed in nature and forms at least 66 minerals [44]. The major Mo-bearing minerals found in mine wastes are summarised in Table 5. Of these, the most commonly occurring is the sulfide molybdenite. This occurs as a major component in mine wastes of Mo- and Cu-Mo porphyry deposits [33,45,46], epithermal Au and Au-Ag-(Te) deposits [32] and W-Mo porphyry-greisen deposits [47]. Molybdenite often occurs with other sulfide minerals, including pyrite and chalcopyrite (e.g., in sediments associated with waste-water effluents from the concentration plants of Sarcheshmeh Cu mine, SE Iran [31]). The proportion of molybdenite in mine wastes varies from traces [32,33,46] to approximately 1% of the total mineral composition [31,48]. For example, Xu et al. [49] used X-ray diffraction (XRD) to show that molybdenite was the second most abundant sulfide (<1% of total minerals) after pyrite (<3% of total minerals) in tailings in the Lanjiagou mining area, China. Molybdenite was also detected in three boreholes in the same area, but only in the water-saturated zone between 160 and 200 cm depth. Dold and Fontboté [33] found trace molybdenite in the upper parts of the Piuquenes tailings impoundment at La Andina, Chile.

The oxidation of molybdenite in weathered porphyry deposits can result in the formation of a number of secondary minerals, such as ferrimolybdate [34]. Langedal [50] suggested that an important part of the reducible fraction of Mo in Knaben Molybdenum Mines tailings, Norway, is represented by molybdate fixed in ferrimolybdite. Originally, powellite was not considered to be a significant sink for molydate due to its high solubility in surface waters [50,51]. Despite this, batch experiments and field cell samples have showed that this mineral can be an important secondary sink for Mo in pH neutral mine waste waters. Powellite forms as coatings on carbonates and silicate minerals, or in association with molybdenite, but the process is proposed to be kinetically limited. After the

nucleation phase, powellite formation from supersaturated conditions is proposed to follow a second order rate expression with linear dependence on $[Ca^{2+}]$ and $[MoO_4^{2-}]$ [52,53]. Consequently, powellite formation is thought to depend on the residence time of the water and its enrichment with sufficient Mo and Ca for precipitation.

X-ray absorption near-edge structure (XANES) absorption spectroscopy analysis of the uranium Deilmann Tailings Management Facility (TMF) in northern Saskatchewan, Canada, showed that Mo occurred as varying proportions of solid $NiMoO_4$ and $CaMoO_4$ complexes, as well as molybdate adsorbed on ferrihydrite [54]. Tailings samples with low Fe/Mo (<708) and high Ni/Mo (>113) molar ratios are dominated by $NiMoO_4$, otherwise they are dominated by molybdate adsorbed on ferrihydrite. This contrasts with another northern Saskatchewan TMF (the JEB TMF) that operates at lower pH (7.3) and in which Mo (25–505 mg/kg in tailings) exists primarily as powellite, ferrimolybdenite and molybdate adsorbed on ferrihydrite [55,56]. However, rapid changes in the Mo mineralogy occurred in the first five years of the emplacement of tailings in the TFM [56]. Ferrimolybdate and molybdate-sorbed ferrihydrite were shown to dissolve (Figure 2), liberating molybdate. Subsequently, Mo precipitated as powellite (from 10% of the Mo species in 2008 to 25% in 2013), and this mineral was then proposed to control the long-term stability of Mo in the pore waters [56].

Table 5. Mo-bearing minerals in mine wastes.

Mineral	Composition	References
Ferrihydrite	$(Fe^{3+})_2O_3 \cdot 0.5H_2O$	Essilfie-Dughan et al. [54]; Hayes et al. [55]; Blanchard et al. [56]
Ferrimolybdite	$Fe_2(MoO_4)_3 \cdot 7H_2O$	Langedal [50]; Hayes et al. [55]; Blanchard et al. [56]
Jorsidite	MoS_2	Dold and Fontboté [33]; Dold and Fontbotè [57]
Molybdenite	MoS_2	Abrosimova et al. [45]; Sima et al. [32]; Smuda et al. [9,34]; Yu et al. [46]; Langedal [50]; Khorasanipour et al. [31]; Petrunic and al [47]; Petrunic et al. [58]; Blanchard et al. [56]
Molybdite	MoO_3	Abrosimova et al. [45]
Nickel(II) molybdate	$NiMoO_4$	Essilfie-Dughan et al. [54]
Powellite	$CaMO_4$	Conlan et al. [53]; Langedal [50]; Hayes et al. [55]; Blanchard et al. [56]
Tugarinovite	MoO_2	Abrosimova et al. [45]
Wulfenite	$PbMoO_4$	Conlan et al. [53]; Petrunic et al. [58]; Petrunic [59]

Batch experiments simulating conditions and chemicals expected in the Antamina waste-rock piles, Peru, including Mo, SO_4 and calcite, demonstrated that wulfenite formed almost instantaneously and more rapidly that powellite, with Pb concentrations dropping to below detection limits within 15 min. The significance of wulfenite at mine sites has been suggested to be limited by the availability of Pb [53]. Langedal [50], for example, observed that in Knaben Molybdenum mines tailings wulfenite is not likely to be an important Mo sink due to low Pb concentrations (6 ppm). Nevertheless, Petrunic et al. [58] observed secondary wulfenite accompanied by an unidentified Bi-Pb-As-O phase in pH 9 mine tailings, in the interstitial voids present in a Fe-Zn-As-O phase and in close proximity to molybdenite grains [59]. Primary wulfenite was also detected by scanning electron microscopy with energy-dispersive X-ray spectroscopy (SEM-EDS) analysis and considered the main Mo-bearing bearing mineral in four mine waste Pb-Zn ore deposits in the Meža Valley, Slovenia, with a relative abundance <5 vol. %, mostly in the form of individual grains varying between 4.1 and 12.1 μm in diameter, or associated with carbonates [43]. Additionally, results from Mo-bearing coal overburden in the Powder River Basin, Wyoming, suggest that dissolved Mo concentrations in mine spoils and soils near the mine may be controlled by a $PbMoO_4$ solid phase [42]. Powellite and wulfenite precipitation are not affected by high concentrations of Cu and Zn, which may be expected in many mine waste contexts, even when supersaturation of Cu and Zn molybdates is predicted [53]. A column experiment performed to investigate Mo attenuation with aqueous Pb, Cu and Zn under flow conditions showed that, in contrast to Pb and Ca, both Cu and Zn did not form distinct molybdate precipitates [53].

Tugarinovite and molybdite were identified through X-ray diffraction (XRD) analysis by Abrosimova et al. [45] in a waste rock sample containing several oxidized grains at the Ak-Sug porphyry Cu-Mo deposit, Russia. A Mo oxide with an MoO_3 composition typical of molybdite was also found in minor amounts (1.92% of the total Mo-bearing mineral composition, with the remaining 98.08% as Mo sulfide) in ultrafine tailings from an obsolete molybdenite reservoir in Zhejiang province, China [48].
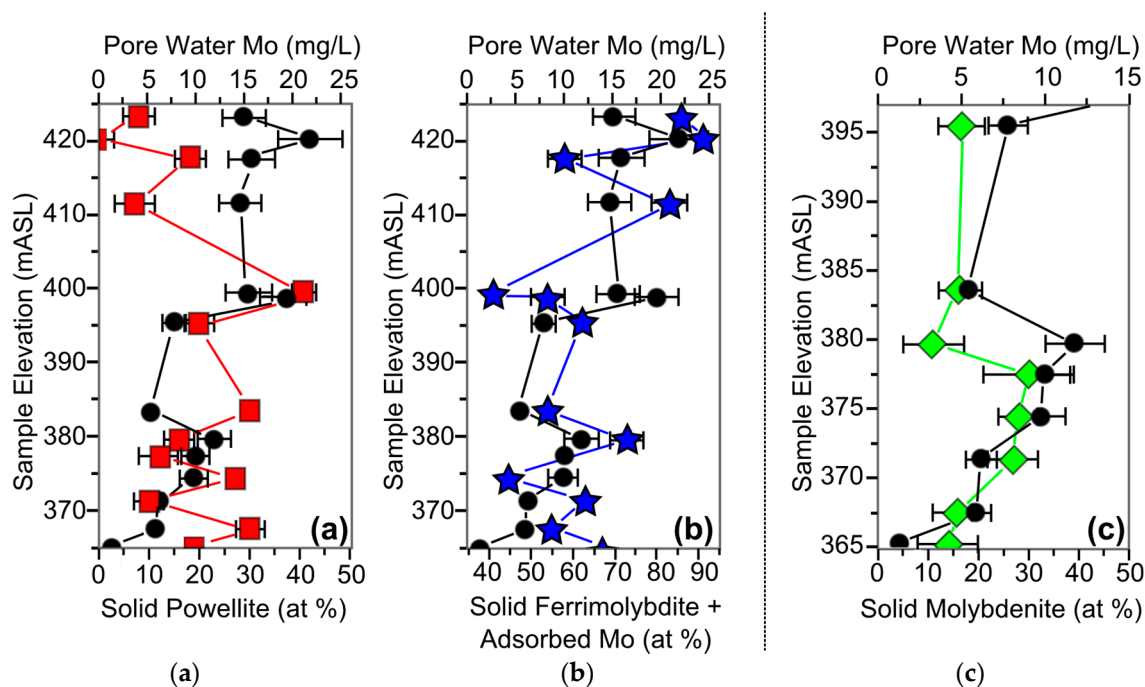

Figure 2. Aqueous Mo pore water concentrations (black lines) compared to relative amounts of solid (**a**) powellite (red line), (**b**) ferrimolybdite and molybdate adsorbed on ferrihydrite (blue line) and (**c**) molybdenite (green line). Errors in the Mo pore water concentrations are c. 15% for concentrations >1 mg/L. Error bars are only shown where they exceed the size of the symbol. A dashed line separates plot (**c**) because of the different sample elevation for this plot relative to plots (**a**,**b**). Data are taken from borehole TMF 13-01 from the uranium mining operation JEB Tailings Management Facility, Saskatchewan, Canada. Reprinted (adapted) with permission from Blanchard et al. [56]. Copyright (2015) American Chemical Society.

It has been proposed that molybdate can be taken up in a wide range of secondary minerals, including kornelite, magnesiocopiapite, coquimbite and hydronium jarosite in mine tailings [31,33]. Table 6 presents a summary of mine waste minerals in which Mo is reported or suggested to occur as a trace element. Of these, pyrite is the most abundant and has been shown to contain between 2.2 and 790 mg/kg (ppm) of Mo, possibly entering in the pyrite lattice via non stoichiometric substitution during mineral formation [60]. Roasted pyrite in tailings in the Aljustrel mining area, Portugal, has been shown to be enriched in Mo (31.2 mg/kg [61]), while coarse pyrite was more enriched in Fe, Cu, Pb and other metals (3.4 to 15.8 mg/kg of Mo). The Mo (49.5–76.3 mg/kg) detected in mine tailings at the Greens Creek Mine, Alaska, has also been attributed to its occurrence in pyrite [39]. Molybdenum is also suggested to occur in other mine waste sulfides (e.g., chalcopyrite, pyrrhotite and sphalerite [62,63]), but concentration data are available only for galena (7 ppm [64]) and tetrahedrite (0.8 wt % [65]). Khorasanipour and Eslami [66] suggested pyrite and chalcopyrite as hosts of Mo in the unoxidised tailings at the Sarcheshmeh porphyry Cu mine, Iran, mainly in the form of non-leachable fraction (0.01–0.65 mg/kg for the Toxicity Characteristic Leaching Procedure (TCLP) and >100 mg/kg for total concentration).

Several studies have reported that Mo is strongly associated with Fe(III) oxyhydroxides in acid oxidising mine wastes (Table 6; [33,67]). Under such conditions, Mo occurs as a negatively charged species (e.g., molybdate [68]), whereas Fe(III) (oxy)hydroxide surfaces exhibit net positive charge [69]. As a result, the formation of inner sphere complexes with these surfaces has been proposed to be an important control on Mo mobility within tailings deposits [10,39], and an effective removal technique for remediating Mo-contaminated mine waters [31,33,70,71].

Table 6. Minerals in mine wastes containing Mo as a trace element.

Mineral	Composition	References
Fe oxyhydroxides	$FeOOH$	Favas et al. [28]; Holmstrom and Ohlander [72]; Romero et al. [63]; Khorasanipour et al. [31]; Khorasanipour and Eslami [66]
Pyrite	FeS_2	Lindsay et al. [39]; Candeias et al. [61]; Khorasanipour et al. [31]; Khorasanipour and Eslami [66,70]; Khorasanipour [71]
Chalcopyrite	$CuFeS_2$	Khorasanipour and Eslami [66,70]; Khorasanipour et al. [31]; Khorasanipour [71]
Jarosite	$KFe_3(OH)_6(SO_4)_2$	Romero et al. [73]; Smuda et al. [34]; Khorasanipour [71]
Schwertmannite	$Fe_8O_8(OH)_6(SO_4)\cdot nH_2O$	Dold and Fontboté [33]

* Inferred from sequential extractions.

In many mine waste studies the mineralogy of Mo is inferred from sequential extraction data rather than determined directly. A series of sequential extraction schemes for Mo have been developed, and these are outlined in Table 7. The number of steps in the schemes increase with age of the study, from 4 [50] to 7 [33] to 9 [31]. All of the schemes extract bioavailable, exchangeable (adsorbed), oxidisable (sulfides and organic matter) and residual Mo. The Dold and Fontboté [33] and Khorasanipour et al. [31] schemes additionally extract a carbonate phase and a reducible (Fe oxide) phase, and they separate the organic and sulfide phases. As such, some of the steps of the schemes are designed to extract specific minerals.

In tailings and soils surrounding the abandoned Sn-As Ervedosa Mine, Portugal, the easily reducible fraction, which represents metals bound to short range-order Fe, Al and Mn (oxy)hydroxides and poorly-crystallised ferric hydroxysulfates, accounted for the 0.0%–80.1% of the total Mo extracted. The moderately reducible fraction, representing metals bound to long-range-order Fe, Al and Mn (oxy) hydroxides and well-crystallised ferric hydroxysulfates, accounted for the 5.8%–100% of the total Mo [28]. Molybdenum was also extracted in the primary sulfide (0.0%–43.76%), organic matter (0.0%–7.1%) and residual fractions (0.0%–19.9%). In Stekenjokk Cu-Zn mine tailings, Sweden, 55%–66% of the total Mo is reported as non-sulfide bound, which was suggested to represent Fe and Mn-oxyhydroxides and organic material [72]. Smuda et al. [34] also reported high Mo and Fe concentrations in the low- and high-crystalline Fe(III) oxyhydroxide fraction. They suggested that this represented the typical secondary minerals jarosite and poorly crystalline Fe oxyhydroxides found in the oxidation zones in tailings.

The Fe(III) hydroxysulfate schwertmannite, a ubiquitous mineral formed from acid rock drainage (ARD) and acid mine drainage (AMD), has been suggested to potentially be an important sink for Mo [74–77]. Its importance in retaining the molybdate oxyanion in the low pH oxidation zone of tailings was highlighted by Dold and Fontboté [33] through a seven-step sequential extraction and electron microprobe analysis (EPMA). However, schwertmannite is metastable and transforms into jarosite and goethite with time [75], but these minerals are also proposed to take up Mo (Table 7).

The chemically-defined residual fraction has been attributed to Mo associated with silicate minerals. For example, a large residual fraction (11%–42% of Mo) in mine tailings from the Knaben Molybdenum Mines, Sweden, was attributed to Mo-bearing micas and amphiboles [50]. High Mo concentrations (2.670 µg/L) in alkaline tailings waters of the Talabre tailings impoundment, Chuquicamata mine, Chile, were attributed to desorption from clay minerals [34].

Table 7. Sequential extraction schemes for Mo in mine wastes.

	Langedal [50]			Dold and Fontboté [33]			Khorasanipour et al. [31]
	Fraction: Reagents	**Mineral Attribution**		**Fraction: Reagents**	**Mineral Attribution**		**Fraction: Reagents**
(1)	Bioavailable: 30 mL 0.01 M BaCl$_2$		(1)	Water soluble: 1 g of sample into 50 mL of deionized H$_2$0, shake for 1 h	water-soluble sulfates, e.g., gy, bonattite, chalcantite	(1)	Water soluble: 1 g of air dried solid sample into 50 mL of de-ionized H$_2$O and shaken for 2 h at room temperature
(2)	Adsorbed/ion exchangeable: 30 mL 1 M NH$_4$OA		(2)	Exchangeable: 1 M NH$_4$-Acetate pH 4.5, shake for 2 h at room temperature	ca, vermiculite-type-mixed-layer, exchangeable ions	(2)	Exchangeable: 1 M NH$_4$OAc at pH 7, continuous shaking for 2 h at room temperature
						(3)	Acid-soluble or carbonates: at room temperature with a 50 mL buffered acetic acid/sodium acetate solution (adjusted to pH 5 with HOAc) for 4 h, with continuous stirring.
						(4)	Reducible: 40 mL oxalic acid /ammonium oxalate
			(3)	Fe(III)oxy-hydroxides: 0.2 M NH$_4$-oxalate pH 3.0, shake for 1 h in darkness	sh, 2-line fh, secondary jt, MnO$_2$	(5)	amorphous Fe oxides: 50 mL of 0.2 M NH$_4$ oxalate (NH$_4$C$_2$O$_4$), adjusted to pH 3 with 0.2-M oxalic acid (H$_2$C$_2$O$_4$), and shaken for 4 h in darkness at ambient temperature.
			(4)	Fe(III)oxides: 0.2 M NH$_4$-oxalate pH3.0, heat in water bath 80°C for 2 h	gt, jt, Na-jt, hm, mt, higher ordered fh	(6)	crystalline Fe oxide phases: 50 mL of 0.2 M NH$_4$C$_2$O$_4$, adjusted to pH 3.3 with a 0.1-M solution of ascorbic acid, at 100 °C for 30 min.
(3)	Oxidisable: (a) 10 mL 30% H$_2$0$_2$; (b) 40 mL 1 M NH$_4$OAc	Sulfides, organic matter	(5)	Organics and secondary Cu-sulfides: H$_2$O$_2$ 35%, heat in water bath for 1h	organic, cv, cc-, dg	(7)	Oxidisable (organic matter): 30% H$_2$O$_2$ (adjusted to pH 2 by use of 0.02-M HNO$_3$), and continuously shaken for 3 h at 85 °C.
			(6)	Primary sulfides: Combination of KClO$_3$ and HCl, followed by 4 M HNO$_3$ boiling	py, cp, cc, bn, sl, gn, tt, cb, op, stbp	(8)	Primary sulfides: combination of KClO$_3$ and HCl, followed by 4 M HNO$_3$ at boiling point.
(5)	Residual: 2.6 mL HCl + 0.9 mL HNO$_3$	Micas, amphiboles	(7)	Residual: HNO$_3$, HF, HClO$_4$, HCl digestion	Silicates	(9)	Residual: digestion with HNO$_3$, HClO$_4$, HF and HCl.

4. Microbiology of Molybdenum in Mine Wastes

Bryner and Anderson [78] demonstrated that molybdenite can be bioleached by autotrophic bacteria. *Acidithiobacillus ferrooxidans* and *T. thiooxidans* isolated from drainage from Kennecott's open-pit mine in Bingham Canyon, Utah, USA, were shown to be capable of oxidising molybdenite, but only in the presence of pyrite. This oxidation process generated molybdate, which was thought to be poisonous to *At. Ferrooxidans* [78–80]. However, little work was done after this time that due to the reported resistance of molybdenite to biooxidation and the toxicity of molybdate to the bacteria, and the authors suggested that commercial bioleaching was not practical [81,82].

Acidithiobacillus ferrooxidans exhibits a remarkable tolerance to most metal cations (Cu^{2+}, Cd, Cr). However, molybdenum oxide inhibits cell growth and the iron-oxidising activity in concentrations $>10^{-3}$ M [83]. A Mo(V) resistance mechanism in *At. ferrooxidans* was reported by Yong et al. [84] for the strain Funis2-1 among seventy five strains of iron-oxidising bacteria isolated from streams and soils in Japan and USA. Mo(VI) is chemically reduced by Fe(II) to give Fe(III) and Mo(V), and the Mo(V) formed binds to the plasma membrane, probably to the cytochrome-c oxidase (lowering its activity), inhibiting Fe(II) oxidation and consequently growth. Resistance is based on a combination of a cytochrome-c oxidase that is tolerant to higher concentrations of Mo(V) and on an Mo(V)-oxidizing activity sixfold greater than that detected in the sensitive *At. ferrooxidans* strain AP19-3. *Leptospirillum ferrooxidans* tolerates lower pH values and higher concentrations of U, Mo and Ag than *At. ferrooxidans*, but it is more sensitive to copper and is unable to oxidize sulfur or sulfur compounds [85]. Therefore, sulfide minerals can be attacked by *L. ferrooxidans* only together with *T. ferrooxidans* or *T. thiooxidans*.

Some case studies involving bacteria and Mo-bearing mine wastes have been carried out. For example, Dold and Fontbotè [33] observed an enrichment of Mo in the organic fraction of the oxidation zone below a hematite-rich seam in the Piquenes tailing impoundment, El Teniente (27 ppm). They suggested that this enrichment depended on Mo fixation in dead cell material of sulfide oxidising bacteria (e.g., *T. Ferrooxidans*). The enriched horizon is coarser than the surroundings, with a higher possibility of O_2 transport, resulting in higher aerobic activity, increased molybdenite oxidation and potential negative effects on sulfide-oxidizing bacteria.

Growth assays revealed that 22 of the 199 bacterial isolates obtained from Deillman Tailings Facility (DTMF), Canada, had the ability to reduce molybdate [86]. Biofilms grown nearest to alkaline uranium mine tailings at the same facility had concentrations approximately 5× higher (0.042 μg for 1 cm² polycarbonate coupons) compared to biofilms from 1 m depth (0.008 μg for 1 cm² polycarbonate coupons). Dissolved Mo concentrations increased with depth in the water column [87], and the elevated concentrations of Mo, V and Pb at lower depths were suggested to be due to the effect of the alkaline pH.

Kauffman et al. [88] completed the first in-situ biorestoration experiment. For this, the percolation of uranium mine discharge water through Ambrosia Lake soil, NM, USA, lowered Se, U, Mo and SO_4 concentrations in U mine waters (from 0.05 to 1.90 mg/L to 0.5, 0.1, 0.05 and 600 mg/L, respectively) by the activity of *Clostridium* sp. and sulfate-reducing bacteria. However, the Mo content was sharply reduced only after the addition of sucrose. The removal mechanism was proposed to be the reaction of hydrogen sulfide, produced as a result of sulfate reduction by *Desulfovibrio*, with uranyl and molybdate ions to form insoluble uranium and molybdenum species.

No studies have been found to date in which Mo-metabolising bacteria have been isolated from mine wastes. However, laboratory experiments on other types of contaminated land involving Mo-reducing and -oxidising bacteria have been carried out. According to Levine [89], the first mention of the microbial reduction (by *E. coli*) of molybdenum (VI) to molybdenum blue (V) was reported by Capaldi and Proskauer [90]. Most of the Mo-reducing bacteria isolated to date are from Malaysian soils [91,92], where Mo is produced as a by-product of copper from a mine in Sabah [91]. Isolation of Mo-reducing bacteria is also reported for soils from Pakistan [93], Sudan (*Enterobacter sp. strain Zeid-6* [94]), Indonesia [95] and Antarctica (*Pseudomonas sp. strain DRY1* [96]). The majority of

molybdenum-reducing bacteria identified so far are gram negative, with the exception of *Bacillus* sp. Strain Lbna, a genus that shows extreme environmental tolerance due to its ability to form endospores and with a fast doubling time, and hence a good bioremediating agent [97].

In all of the Mo-reducing bacteria studied to date, phosphate concentrations higher than 5 mM inhibited molybdate reduction. Phosphomolybdate has an important intermediary role during molybdate reduction, but this complex is disrupted by phosphate, preventing reduction to Mo-blue [98]. The bacteria are capable of appreciable reduction of molybdate if soil phosphate concentrations do not exceed 20 mM [98], which is rarely the case. The activity of the Mo-reducing bacteria studied is also inhibited to varying degrees by different metallic elements, as is reported for other metal-reducing bacteria, and it generally indicates an enzymatic rather than abiotic origin [97]. Khan et al. [93] isolated several Mo-reducing bacteria from Pakistani soils, some of them showing a resistance to high Mo concentrations (up to 50 mM) while others showed better resistance to metals such as Cu and Hg.

5. Geochemical-Mineralogical-Microbiological Controls on Molybdenum Mobility in Mining-Affected Environments

Mining of Mo-rich deposits and of deposits containing Mo as a trace metal has led to enrichment of water, soil and plants in Mo (Tables 1–4). Mo concentrations in mine tailings vary widely, from <100 mg/kg Mo to nearly 4000 mg/kg Mo (Table 2), with the highest concentrations recorded for Cu- and Cu-Mo-porphyry mines. The highest Mo aqueous concentrations recorded in mining-affected environments occur in tailings impoundments and in acid to slightly alkaline mine drainage (Table 1). By contrast, Mo concentrations in mining-affected soils and sediments are often below global background concentrations for soils (10 mg/kg), but elevated concentrations of between 100 and 200 mg/kg are recorded, generally near tailings impoundments or in fluvial sediments downstream of mining areas (Table 3). The two studies on Mo uptake in mining-affected plants discussed in this review suggest that some are able to exclude Mo from their roots and shoots (e.g., *Cistus*, *Quercus* species), whereas others take up Mo yet thrive (e.g., *Baccharis* species) (Table 4). It is clear, however, that there is an overall lack of data of geochemistry of Mo in mining-affected environments. To our knowledge, there are no data on the impact of mining-related Mo on dusts or animals (including humans).

The main types of Mo-bearing minerals found to date in mine wastes, and the geochemical relationships between them, are summarised schematically in Figure 3. The main ore mineral of Mo, molybdenite, has been shown to be stable in acidic environments [19,52], but it undergoes oxidative dissolution under atmospheric conditions and neutral to alkaline pH [5,19,53] with liberation of the molybdate oxyanion as follows:

$$2MoS_2 + 9O_2 + 6H_2O \rightarrow 2MoO_4^{2-} + 4SO_4^{2-} + 12H^+ \tag{1}$$

It is assumed that oxidation of other Mo-bearing sulfides, such as pyrite and chalcopyrite, can also result in liberation of Mo and its oxidation to molybdate. Molybdate is stable over a wide range of pH conditions, from strongly alkaline down to pH 3–4. In acidic pH waters, the molybdate is protonated to form $HMoO_4^-$ or H_2MoO_4 [5]. Under moderately acidic pH conditions, molybdate can be sorbed onto the secondary Fe(III) minerals (jarosite, schwertmannite, ferrihydrite) that typically form in mining-affected environments [99,100]. These secondary Fe(III) phases can decompose in acidic pH waters (e.g., acid mine drainage), releasing their sorbed molybdate. Molybdate does not tend to sorb to mineral surfaces at neutral pH conditions, and it is taken up in secondary minerals such as powellite and wulfenite at alkaline conditions ([53]; Figure 3). The information shown in Figure 3, therefore, provides baseline information for the distribution and stability of Mo-bearing minerals in mine wastes. It is very possible, however, that other secondary Mo-bearing minerals, such as soluble hydrous Mo sulfate salts, exist. The role of bacteria in forming these minerals is virtually unknown.
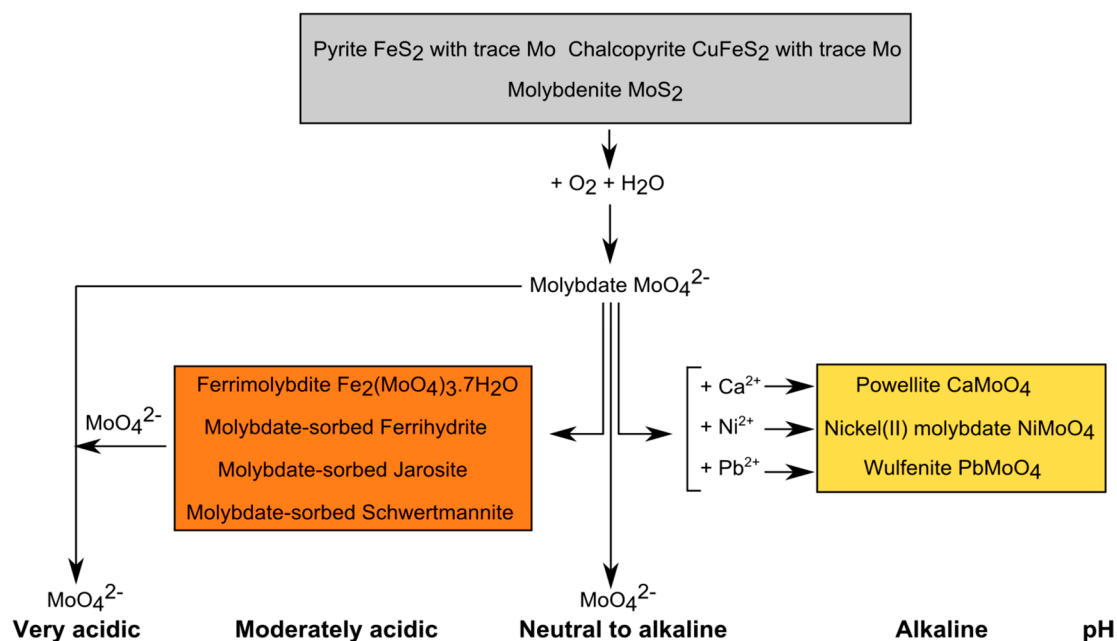
Figure 3. Schematic diagram illustrating the relationships between, and formation of, Mo-bearing minerals in mine wastes. Solid minerals are shown in boxes, and relationships between them involving aqueous species are shown with arrows. The pH conditions under which the minerals and aqueous species are stable are indicated at the bottom of the figure.

6. Conclusions

This review summarises available data and outlines our present understanding of the geochemistry, mineralogy and microbiology of Mo in mine wastes. Although previous studies have provided a framework for understanding the distribution and environmental impact of Mo in mining-affected environments, there is clearly a need for much further research. In particular, further substantive data on the concentrations of Mo in mine wastes, and mining-affected water, soils, dusts, plants and animals, are needed. Studies focusing on the impact of mining-related Mo on human health, the character and stability of secondary Mo-bearing minerals produced by mine waste weathering, and the role of bacteria and other microorganisms in the cycling of mining-related Mo would provide knowledge to underpin management and remediation schemes for Mo-affected mining environments.

References

1.　Kropschot, S.J. Molybdenum—A Key Component Of Metal Alloys. USGS Mineral Resources Program Fact Sheet 2009-3106; 2010. Available online: https://pubs.usgs.gov/fs/2009/3106/ (accessed on 23 January 2018).

2.　International Molybdenum Association (IMOA). Molybdenum Ore Reserves. Available online: http://www.imoa.info/molybdenum/molybdenum-ore-reserves.php (accessed on 9 November 2017).

3.　Polyak, D.E. Molybdenum. Available online: https://minerals.usgs.gov/minerals/pubs/commodity/molybdenum/mcs-2017-molyb.pdf (accessed on 16 October 2017).

4.　National Academy of Sciences. *Recommended Dietary Allowances*, 10th ed.; National Academy Press: Washington, DC, USA, 1989.

5.   Smedley, P.L.; Kinniburgh, D.G. Molybdenum in natural waters: A review of occurrence, distributions and controls. *Appl. Geochem.* **2017**, *84*, 387–432. [CrossRef]

6.   Chudy, K.; Marszałek, H.; Kierczak, J. Impact of hard-coal waste dump on water quality—A case study of Ludwikowice Kłodzkie (Nowa Ruda Coalfield, SW Poland). *J. Geochem. Explor.* **2014**, *146*, 127–135. [CrossRef]

7.   Sánchez España, J.; González Toril, E.; López Pamo, E.; Amils, R.; Diez Ercilla, M.; Santofimia Pastor, E.; San Martín-Úriz, P. Biogeochemistry of a hyperacidic and ultraconcentrated pyrite leachate in San Telmo mine (Iberian Pyrite Belt, Spain). *Water Air Soil Pollut.* **2008**, *194*, 243–257. [CrossRef]

8.   Skierszkan, E.K.; Mayer, K.U.; Weis, D.; Beckie, R.D. Molybdenum and zinc stable isotope variation in mining waste rock drainage and waste rock at the Antamina mine, Peru. *Sci. Total Environ.* **2016**, *550*, 103–113. [CrossRef] [PubMed]

9.   Smuda, J.; Dold, B.; Spangenberg, J.E.; Pfeifer, H.-R. Geochemistry and stable isotope composition of fresh alkaline porphyry copper tailings: Implications on sources and mobility of elements during transport and early stages of deposition. *Chem. Geol.* **2008**, *256*, 62–76. [CrossRef]

10. Lindsay, M.B.J.; Moncur, M.C.; Bain, J.G.; Jambor, J.L.; Ptacek, C.J.; Blowes, D.W. Geochemical and mineralogical aspects of sulfide mine tailings. *Appl. Geochem.* **2015**, *57*, 157–177. [CrossRef]

11. Parviainen, A.; Isoaari, P.; Loukola-Ruskeeniemi, K.; Nieto, J.M.; Gervilla, F. Occurrence and mobility of As in the Ylöjärbi Cu-W-As mine tailings. *J. Geochem. Explor.* **2012**, *114*, 36–45. [CrossRef]

12. Wurl, J.; Mendez-Rodriguez, L.; Acosta-Vargas, B. Arsenic content in groundwater from the southern part of the San Antonio-El Triunfo mining district, Baja California Sur, Mexico. *J. Hydrol.* **2014**, *518*, 447–459. [CrossRef]

13. Alakangas, L.; Öhander, B.; Lundberg, A. Estimation of temporal changes in oxidation rates of sulphides in copper mine tailings at Laver, Northern Sweden. *Sci. Total Environ.* **2010**, *408*, 1386–1392. [CrossRef] [PubMed]

14. Huang, S.; Sillanpää, M.; Gjessing, E.T.; Peräniemi, S.; Vogt, R.D. Environmental impact of mining activities on the surface water quality in Tibet: Gyama valley. *Sci. Total Environ.* **2010**, *408*, 4177–4184. [CrossRef] [PubMed]

15. Miller, C.A.; Peucker-Ehrenbrink, B.; Walker, B.D.; Marcantonio, F. Re-assessing the surface cycling of molybdenum and rhenium. *Geochim. Cosmochim. Acta* **2011**, *75*, 7146–7179. [CrossRef]

16. Emerson, S.R.; Huested, S.S. Ocean anoxia and the concentrations of molybdenum and vanadium in seawater. *Mar. Chem.* **1991**, *34*, 177–196. [CrossRef]

17. Greber, N.D.; Mäder, U.; Nägler, T. Experimental dissolution of molybdenum-sulphides at low oxygen concentrations: A first-order approximation of late Archean atmospheric conditions. *Earth Space Sci.* **2015**, *2*, 173–180. [CrossRef]

18. World Health Organization (WHO). *Molybdenum in Drinking Water*; Background Document for Development of WHO Guidelines for Drinking-Water Quality; World Health Organization: Geneva, Switzerland, 2011.

19. Xu, N.; Braida, W.; Christodoulatos, C.; Chen, J. A Review of Molybdenum Adsorption in Soils/Bed Sediments: Speciation, Mechanism, and Model Applications. *Soil Sediment Contam.* **2013**, *22*, 912–929. [CrossRef]

20. Matthies, R.; Sinclair, S.A.; Blowes, D.W. The zinc stable isotope signature of waster rock drainage in the Canadian permafrost region. *Appl. Geochem.* **2014**, *48*, 53–57. [CrossRef]

21. Aykol, A.; Budakoglu, M.; Kumral, M.; Gultekin, A.H.; Turhan, M.; Esenli, V.; Yavuz, F.; Orgun, Y. Heavy metal pollution and acid drainage from the abandoned Balya Pb-Zn sulfide Mine, NW Anatolia, Turkey. *Environ. Geol.* **2003**, *45*, 198–208. [CrossRef]

22. U.S. Department of the Interior. *Water Quality Criteria: Report of the National Technical Advisory Committee to the Secretary of the Interior*; Federal Water Pollution Control Administration: Washington, DC, USA, 1968.

23. SEPA & AQSIQ (State Environmental Protection Administration of the P.R. China & General Administration of Quality Supervision, Inspection and Quarantine of the P.R. China). *Chinese National Standards GB 3838-2002: Environmental Quality Standards for Surface Water*; Ministry of environmental protection of the People's Republic of China: Beijing, China, 2002. (In Chinese)

24. CCME. *Canadian Environmental Quality Guidelines*; Canadian Council of Ministers of the Environment: Ottawa, ON, Canada, 2007. Available online: http://www.ccme.ca/en/resources/canadian_environmental_quality_guidelines/index.html (accessed on 8 August 2017).

25. U.S. EPA. *Standards for Remedial Actions at Inactive Uranium Processing Sites, Federal Register*; 40 CFR Part 192; U.S. Environmental Protection Agency: Washington, DC, USA, 1987.

26. Rudnick, R.L.; Gao, S. Composition of the continental crust. In *Treatise on Geochemistry*, 1st ed.; Elsevier: Amsterdam, The Nederland, 2003.

27. Farago, M.E.; Cole, M.; Xiao, X.; Vaz, M.C. Preliminary assessment of metal bioavailability to plants in the Neves Corvo area of Portugal. *Chem. Spec. Bioavail.* **1992**, *4*, 19–27. [CrossRef]

28. Favas, P.J.C.; Pratas, J.; Gomes, M.E.P.; Cala, V. Selective chemical extraction of heavy metals in tailings and soils contaminated by mining activity: Environmental implications. *J. Geochem. Explor.* **2011**, *111*, 160–171. [CrossRef]

29. Candeias, C.; Melo, R.; Ávila, P.F.; Ferreira da Silva, E.; Salgueiro, A.R.; Teixeira, J.P. Heavy metal pollution in mine-soil-plant system in S. Francisco de Assis—Panasqueira mine (Portugal). *Appl. Geochem.* **2014**, *44*, 12–26. [CrossRef]

30. Khorasanipour, M.; Esmaeilzadeh, E. Environmental characterisation of Sarcheshmeh Cu-smelting slag, Kerman, Iran: Application of geochemistry, mineralogy and single extraction methods. *J. Geochem. Explor.* **2016**, *166*, 1–17. [CrossRef]

31. Khorasanipour, M.; Tangestani, M.H.; Naseh, R.; Majmohammadi, H. Hydrochemistry, mineralogy and chemical fractionation of mine and processing wastes associated with porphyry copper mines: A case study from the Sarcheshmeh mine, Iran. *Appl. Geochem.* **2011**, *26*, 714–730. [CrossRef]

32. Sima, M.; Dold, B.; Frie, L.; Senila, M.; Balteanu, D.; Zobrist, J. Sulfide oxidation and acid mine drainage formation within two active tailings impoundments in the Golden Quadrangle of the Apuseni Mountains, Romania. *J. Hazard. Mat.* **2011**, *189*, 624–639. [CrossRef] [PubMed]

33. Dold, B.; Fontboté, L. Element cycling and secondary mineralogy in porphyry copper tailings as a function of climate, primary mineralogy, and mineral processing. *J. Geochem. Explor.* **2001**, *74*, 3–55. [CrossRef]

34. Smuda, J.; Dold, B.; Spangenberg, J.E.; Friese, K.; Kobek, M.R.; Bustos, C.A.; Pfeifer, H.-R. Element cycling during the transition from alkaline to acidic environment in an active porphyry copper tailings impoundment, Chuquicamata, Chile. *J. Geochem. Explor.* **2014**, *140*, 23–40. [CrossRef]

35. Kelm, U.; Helle, S.; Matthies, R.; Morales, A. Distribution of trace elements in soils surrounding the El Teniente porphyry copper deposit, Chile: The influence of smelter emissions and a tailings deposit. *Environ. Geol.* **2009**, *57*, 365–376. [CrossRef]

36. Pérez Rodríguez, N.; Engström, E.; Rodushkin, I.; Nason, P.; Alakangas, L.; Öhander, B. Copper and iron isotope fractionation in mine tailings at the Laver and Kristineberg mines, northern Sweden. *Appl. Geochem.* **2013**, *32*, 204–215. [CrossRef]

37. Holmström, H.; Salmon, U.J.; Carlsson, E.; Petrov, P.; Öhlander, B. Geochemical investigations of sulfide-bearing tailings at Kristineberg, northern Sweden, a few years after remediation. *Sci. Total Environ.* **2001**, *273*, 111–133. [CrossRef]

38. Langedal, M. Dispersion of tailings in the Knabeåna-Kvina drainage basin, Norway, 1: Evaluation of over bank sediments as sampling medium for regional geochemical mapping. *J. Geochem. Explor.* **1997**, *58*, 157–172. [CrossRef]

39. Lindsay, M.B.J.; Condon, P.D.; Jambor, J.L.; Lear, K.G.; Blowes, D.W.; Ptacek, C.J. Mineralogical, geochemical, and microbial investigation of a sulfide-rich tailings deposit characterized by neutral drainage. *Appl. Geochem.* **2009**, *24*, 2212–2221. [CrossRef]

40. Garrido, T.; Mendoza, J.; Arriagada, F. Changes in the sorption, desorption, distribution, and availability of copper, induced by application of sewage sludge on Chilean soils contaminated by mine tailings. *J. Environ. Sci.* **2012**, *24*, 912–918. [CrossRef]

41. Haque, N.; Peralta-Videa, J.R.; Jones, G.L.; Gill, T.E.; Gardea-Torresdey, J.L. Screening the phytoremediation potential of desert broom (*Baccharis sarothroides* Gray) growing on mine tailings in Arizona, USA. *Environ. Pollut.* **2008**, *153*, 362–368. [CrossRef] [PubMed]

42. Wang, L. Geochemical modelling for predicting potential solid phases controlling the dissolved molybdenum in coal overburden, Powder River Basin, WY, U.S.A. *Appl. Geochem.* **1994**, *9*, 37–43. [CrossRef]

43. Miller, M.; Gosar, M. Characteristics and potential environmental influences of mine waste in the area of the closed Mežica Pb-Zn mine (Slovenia). *J. Geochem. Explor.* **2012**, *112*, 152–160. [CrossRef]

44. International Mineralogical Association. Available online: https://www.ima-mineralogy.org (accessed on 30 June 2017).

45. Abrosimova, N.; Gaskova, O.; Loshkareva, A.; Edelev, A.; Bortnikova, S. Assessment of the acid mine drainage potential of waste rocks at the Ak-Sug porphyry Co-Mo deposit. *J. Geochem. Explor.* **2015**, *157*, 1–14. [CrossRef]

46. Yu, C.; Xu, S.; Gang, M.; Chen, G.; Zhou, L. Molybdenum pollution and speciation in Never River sediments impacted with Mo mining activities in western Liaoning, northeast China. *Int. J. Environ. Res.* **2011**, *5*, 205–212.

47. Petrunic, B.M.; Al, T.A. Mineral/water interactions in tailings from a tungsten mine, Mount Pleasant, New Brunswick. *Geochim. Cosmochim. Acta* **2005**, *69*, 2469–2483. [CrossRef]

48. Jiangang, F.; Kaida, C.; Hui, W.; Chao, G.; Wei, L. Recovering molybdenite from ultra fine waste tailings by oil agglomerate flotation. *Miner. Eng.* **2012**, *39*, 133–139. [CrossRef]

49. Xu, S.; Yu, C.; Hiroshiro, Y. Migration behaviour of Fe, Cu, Zn, and Mo in alkaline tailings from Lanjiagou porphyry molybdenum deposits, northeast China. *Mem. Fac. Eng. Kyushu Univ.* **2010**, *70*, 19–31.

50. Langedal, M. Dispersion of tailings in the Nabeåna-Kvain drainage basin, Norway, 2: Mobility of Cu and Mo in tailings-derived fluvial sediments. *J. Geochem. Explor.* **1997**, *58*, 173–183. [CrossRef]

51. Wedepohl, K.H. Molybdenum 42. In *Handbook of Geochemistry II-2*; Springer-Verlag Berlin Heidelberg: New York, NY, USA, 1978; ISBN 978-3-642-65935-5.

52. Conlan, M.J.W. Attenuation mechanisms for molybdenum in neutral rock drainage. Master Thesis, University of British Columbia, Vancouver, BC, Canada, 2009.

53. Conlan, M.J.W.; Mayer, K.U.; Blaskovich, R.; Beckie, R.D. Solubility controls for molybdenum in neutral rock drainage. *Geochem. Explor. Environ. Anal.* **2012**, *12*, 21–32. [CrossRef]

54. Essilfie-Dughan, J.; Pickering, I.J.; Hendry, M.J.; George, G.N.; Kotzer, T. Molybdenum speciation in uranium mine tailings using X-ray absorption spectroscopy. *Environ. Sci. Technol.* **2011**, *45*, 455–460. [CrossRef] [PubMed]

55. Hayes, J.R.; Grosvenor, A.P.; Rowson, J.; Hughes, K.; Frey, R.A.; Reid, J. Analysis of the Mo speciation in the JEB tailings management facility at McClean Lake, Saskatchewan. *Environ. Sci. Technol.* **2014**, *48*, 4460–4467. [CrossRef] [PubMed]

56. Blanchard, P.E.R.; Hayes, J.R.; Grosvenor, A.P. Investigating the geochemical model for molybdenum mineralization in the JEB tailings management facility at McClean Lake, Saskatchewan: An X-ray absorption spectroscopy study. *Environ. Sci. Technol.* **2015**, *49*, 6504–6509. [CrossRef] [PubMed]

57. Dold, B.; Fontboté, L. A mineralogical and geochemical study of element mobility in sulfide mine tailings of Fe oxide Cu-Au deposits from the Punta del Cobre belt, northern Chile. *Chem. Geol.* **2002**, *189*, 135–163. [CrossRef]

58. Petrunic, B.M.; Al, T.A.; Weaver, L. A transmission electron microscopy analysis of secondary minerals formed in tungsten-mine tailings with an emphasis on arsenopyrite oxidation. *Appl. Geochem.* **2006**, *21*, 1259–1273. [CrossRef]

59. Petrunic, B.M.; Al, T.A.; Weaver, L.; Hall, D. Identification and characterization of secondary minerals formed in tungsten mine tailings using transmission electron microscopy. *Appl. Geochem.* **2009**, *24*, 2222–2233. [CrossRef]

60. Huston, D.L.; Sie, S.H.; Suter, G.F.; Cooke, D.R.; Both, R.A. Trace elements in sulfide minerals from eastern Australian volcanic-hosted massive sulfide deposits; Part I, Proton microprobe analyses of pyrite, chalcopyrite, and sphalerite, and Part II, Selenium levels in pyrite; comparison with delta 34 S values and implications for the source of sulfur in volcanogenic hydrothermal systems. *Econ. Geol.* **1995**, *90*, 1167–1196. [CrossRef]

61. Candeias, C.; Ferreria da Silva, E.; Salgueiro, A.R.; Pereira, H.G.; Reis, A.P.; Patinha, C.; Matos, J.X.; Ávila, P.H. The use of multivariate statistical analysis of geochemical data for assessing the spatial distribution of soil contamination by potentially toxic elements in the Aljustrel mining area (Iberian Pyrite Belt, Portugal). *Environ. Earth Sci.* **2011**, *62*, 1461–1479. [CrossRef]

62. Vaughan, D.J.; Craig, J.R. *Mineral Chemistry of the Metal Sulfides*; Cambridge University Press: Cambridge, UK, 1978; ISBN 978-0-521-21489-6.

63. Lottermoser, B. *Mine Wastes: Characterization, Treatment and Environmental Impacts*, 1st ed.; Springer: Berlin, Germany, 2003; ISBN 978-3-662-05133-7.

64. Foord, E.E.; Shawe, D.R. The Pb-Bi-Ag-Cu-(Hg) chemistry of galena and some associated sulfosalts. A review and some new data from Colorado California and Pennsylvania. *Can. Mineral.* **1989**, *27*, 363–382.

65. Spiridonov, E.M.; Kachalovskaya, V.M.; Chvileva, T.N. Thallium-bearing hakite, a new fahlore variety. *Trans. USSR Acad. Sci. Earth Sci. Sect.* **1988**, *290*, 206–208.

66. Khorasanipour, M.; Eslami, A. Determination of elements leachability from Sarcheshmeh Porphyry Copper Mine Tailings: Application of toxicity characteristic leaching procedure. *Environ. Process.* **2014**, *1*, 387–403. [CrossRef]

67. Khorasanipour, M.; Tangestani, M.H.; Naseh, R.; Hajmohammadi, H. Chemical fractionation and contamination intensity of trace elements in stream sediments at the Sarcheshmeh Porphyry Copper Mine, SE Iran. *Mine Water Environ.* **2012**, *31*, 199–213. [CrossRef]

68. Dzombak, D.A.; Morel, F.M.M. *Surface Complexation Modeling: Hydrous Ferric Oxide*; Wiley: New York, NY, USA, 1990.

69. Parks, G.A. The isoelectric points of solid oxides, solid hydroxides, and aqueous hydroxo complex systems. *Chem. Rev.* **1965**, *65*, 177–198. [CrossRef]

70. Khorasanipour, M.; Eslami, A. Hydrogeochemistry and contamination of trace elements in Cu-porphyry mine tailings: A case study from the Sarcheshmeh Mine, SE Iran. *Mine Water Environ.* **2014**, *33*, 335–352. [CrossRef]

71. Khorasanipour, M. Environmental mineralogy of Cu-porphyry mine tailings, a case study of semi-arid conditions, Sarcheshmeh mine, SE Iran. *J. Geochem. Explor.* **2015**, *153*, 40–52. [CrossRef]

72. Holmström, H.; Ölander, B. Layers rich in Fe- and Mn-oxyhydroxides formed at the tailings-pond water interface, a possible trap for trace metals in flooded mine tailings. *J. Geochem. Explor.* **2001**, *74*, 189–203. [CrossRef]

73. Romero, A.; González, I.; Galán, E. Estimation of potential pollution of waste mining dumps at Peña del Hierro (Pyrite Belt, SW Spain) as a base for future mitigation actions. *Appl. Geochem.* **2006**, *21*, 1093–1108. [CrossRef]

74. Carlson, L.; Bigham, J.M.; Schwertmann, U.; Kyek, A.; Wagner, F. Scavenging of As from acid mine drainage by schwertmannite and ferrihydrite: A comparison with synthetic analogues. *Environ. Sci. Technol.* **2002**, *36*, 1712–1719. [CrossRef] [PubMed]

75. Acero, P.; Ayora, C.; Torrentó, C.; Nieto, J.-M. The behaviour of trace elements during schwertmannite precipitation and subsequent transformation into goethite and jarosite. *Geochim. Cosmochim. Acta* **2006**, *16*, 4130–4139. [CrossRef]

76. Antelo, J.; Fiol, S.; Gondar, D.; López, R.; Arce, F. Comparison of arsenate, chromate and molybdate binding on schwertmannite: Surface adsorption vs anion-exchange. *J. Colloid Interface Sci.* **2012**, *386*, 338–343. [CrossRef] [PubMed]

77. Antelo, J.; Fiol, S.; Gondar, D.; Pérez, C.; López, R.; Arce, F. Cu(II) incorporation to schwertmannite: Effect on stability and reactivity under AMD conditions. *Geochim. Cosmochim. Acta* **2013**, *119*, 149–163. [CrossRef]

78. Bryner, L.C.; Anderson, R. Microorganisms in leaching sulfide minerals. *Ind. Eng. Chem.* **1957**, *49*, 1721–1724. [CrossRef]

79. Bryner, L.C.; Beck, J.V.; Davis, D.B.; Wilson, D.G. Microorganisms in leaching sulfide minerals. *Ind. Eng. Chem.* **1954**, *46*, 2587–2592. [CrossRef]

80. Bryner, L.C.; Jameson, A.K. Microorganisms in leaching sulfide minerals. *Appl. Microbiol.* **1958**, *6*, 281–287. [PubMed]

81. Duncan, D.W.; Walden, C.C.; Trussell, P.C.; Lowe, E.A. Recent advances in the microbiological leaching of sulfides. *AIME Trans.* **1967**, *238*, 122–128.

82. Tuovinen, O.H.; Kelly, D.P. Biology of Thiobacillus ferrooxidans in relation to the microbiological leaching of sulphide ores. *Z. Allg. Mikrobiol.* **1972**, *12*, 311–346. [CrossRef] [PubMed]

83. Imai, K.; Sugio, T.; Tsuchida, T.; Tano, T. Effect of heavy metal ions on the growth and iron-oxidising activity of *Thiobacillus ferrooxidans*. *Agric. Biol. Chem.* **1975**, *39*, 1349–1354. [CrossRef]

84. Yong, N.K.; Oshima, M.; Blake, R.C.; Sugio, T. Isolation and some properties of an iron-oxidising bacterium *Thiobacillus ferrooxidans* resistant to molybdenum ion. *Biosci. Biotech. Biochem.* **1997**, *61*, 1523–1526. [CrossRef]

85. Bosecker, K. Bioleaching: Metal solubilization by microorganisms. *FEMS Microbiol. Rev.* **1997**, *20*, 591–604. [CrossRef]

86. Bondici, V.F.; Lawrence, J.R.; Khan, N.H.; Hill, J.E.; Yergeau, E.; Wolfaardt, G.M.; Warner, J.; Korber, D.R. Microbial communities in low permeability, high pH uranium mine tailings: Characterization and potential effects. *J. Appl. Microbiol.* **2013**, *114*, 1671–1681. [CrossRef] [PubMed]

87. Bondici, V.F.; Khan, N.H.; Swerhone, G.D.W.; Dynes, J.J.; Lawrence, J.R.; Yergeau, E.; Wolfaardt, G.M.; Warner, J.; Korber, D.R. Biogeochemical activity of microbial biofilms in the water column overlying uranium mine tailings. *J. Appl. Microbiol.* **2014**, *117*, 1079–1094. [CrossRef] [PubMed]

88. Kauffman, J.W.; Laughlin, W.C.; Baldwin, R.A. Microbiological treatment of uranium mine waters. *Environ. Sci. Technol.* **1986**, *20*, 243–248. [CrossRef] [PubMed]

89. Levine, V.E. The reducing properties of microorganisms with special reference to selenium compounds. *J. Bacteriol.* **1925**, *10*, 217–263. [PubMed]

90. Capaldi, A.; Proskauer, B. Beiträge zur Kenntniss der Säurebildung bei Typhus-bacillen und Bacterium coli. *Med. Microbiol. Immunol.* **1896**, *23*, 452–474. [CrossRef]

91. Othman, A.R.; Bakar, N.A.; Halmi, M.I.E.; Johari, W.L.W.; Ahmad, S.A.; Jirangon, H.; Wyed, M.A.; Shukor, M.Y. Kinetics of molybdenum reduction to molybdenum blue by Bacillus sp. Strain A. rzi. *BioMed Res. Int.* **2013**, *2013*, 371058. [CrossRef] [PubMed]

92. Sabullah, M.K.; Rahman, M.F.; Ahmad, S.A.; Sulaiman, M.R.; Shukor, M.S.; Shamaan, N.A.; Shukor, M.Y. Isolation and characterization of a molybdenum-reducing and glyphosate-degrading *Klebsiella oxytoca* Strain Saw-5 in soils from Sarawak. *Agrivita* **2016**, *38*, 1–13. [CrossRef]

93. Khan, A.; Halmi, M.I.E.; Shukor, M.Y. Isolation of Mo-reducing bacterium in soils from Pakistan. *J. Environ. Microbiol. Toxicol.* **2014**, *2*, 38–41.

94. Othman, A.R.; Abu Zeid, I.M.; Rahman, M.F.; Ariffin, F.; Shukor, M.Y. Isolation and characterization of a molybdenum-reducing and orange G-decolorizing Enterobacter sp. strain Zeid-6 in soils from Sudan. *Bioremediat. Sci. Technol. Res.* **2015**, *3*, 13–19.

95. Mansur, R.; Gusmanizar, N.; Roslan, M.A.H.; Ahmad, S.A.; Shukor, M.Y. Isolation and characterisation of a molybdenum-reducing and metanil yellow dye-decolourising *Bacillus* sp. strain Neni-10 in soils from west Sumatera, Indonesia. *Trop. Life Sci. Res.* **2017**, *28*, 69–90. [CrossRef] [PubMed]

96. Ahmad, S.A.; Shukor, M.Y.; Shamaan, N.A.; MacCormack, W.P.; Syed, M.A. Molybdate reduction to molybdenum blue by an Antarctic bacterium. *BioMed Res. Int.* **2013**, *2013*, 871941. [CrossRef] [PubMed]

97. Abo-Shakeer, L.K.A.; Ahmad, S.S.; Shukor, M.Y.; Shamaan, N.A.; Syed, M.A. Isolation and characterization of a molybdenum-reducing *Bacillus pumilus* strain Ibna. *J. Environ. Microbiol. Toxicol.* **2013**, *1*, 9–14.

98. Halmi, M.I.E.; Zuhainis, S.W.; Yusof, M.T.; Shaharuddin, N.A.; Helmi, W.; Shukor, Y.; Syed, M.A.; Ahmad, S.A. Hexavalent molybdenum reduction to Mo-Blue by a sodium-dodecyl-sulfate-degrading *Klebsiella oxytoca* Strain DRY14. *BioMed Res. Int.* **2013**, *2013*, 384541. [CrossRef] [PubMed]

99. Goldberg, S.; Forster, H.S.; Godfrey, C.L. Molybdenum adsorption on oxides, clay minerals, and soils. *Soil Sci. Soc. Am. J.* **1996**, *60*, 425–432. [CrossRef]

100. Xu, N.; Christodoulatos, C.; Braida, W. Adsorption of molybdate and tetrathiomolybdate onto pyrite and goethite: Effect of pH and competitive anions. *Chemosphere* **2006**, *62*, 1726–1735. [CrossRef] [PubMed]